Supporting information

Metal ion-dependent structural phase transition and impact of Jahn-Teller effect in two organic-inorganic hybrid compounds

Shi-Qing Yin, Yu-Qiao Tong, Qian-Jun Gu, Ya-Juan Li, Bo Huang* and Ai-Xin Zhu*

Faculty of Chemistry and Chemical Engineering, Yunnan Normal University, Kunming 650500, China.

Table of Contents

Materials and instrumentations. All chemicals were obtained from commercial sources and used without further purification. Infrared spectra were performed on a Bruker Tensor 27 spectrometer using KBr particles. Powder X-Ray diffraction (PXRD) patterns (Cu-Kα, λ = 1.54056 Å) were collected on a Smartlab9 ϑ–2ϑ diffractometer. Thermogravimetric (TG) analysis was carried out on a Bruker APEX DUO II system at a heating rate of 5 K/min under a N_2 atmosphere. Differential scanning calorimetry (DSC) measurement was performed by cooling-heating the powder sample at a rate of 5 K/min on a TA DSC Q2000 instrument. Single-crystal X-ray data were performed on Bruker D8 VENTURE Ius 3.0 diffractometer with Mo-Kα radiation (λ = 0.71073 Å), and the structures were solved by direct methods and refined by the full-matrix least-squares refinements based on F^2 using the SHELXLTL software package.[1] The complex permittivity ($\varepsilon = \varepsilon' - i\varepsilon''$, ε' is the real part, and ε'' is the imaginary part) were measured using a Tonghui TH2838A LCR meter (applied electric field of 1.0 V) connected to a cryogenic environment controller at a rate of about 3 K/min at various frequencies (1, 2, 4, 6, 8, 10, 20, 40, 60, 80, 100, 200, 400, 600, 800, 10000 kHz). Second harmonic generation (SHG) was measured using a WITec alpha 300RS microscope with a 1064 nm laser. The evolution of the ferroelastic domain was performed in a Leica DM4P polarising microscope.

Synthesis. A water solution containing stoichiometric quantities of dabco (dabco = 1,2-diazabicyclo[2.2.2]octane, 1.12 g, 10 mmol), 30.0 wt% H_2SiF_6 (2.6 mL, 20 mmol), and $MnCO_3$ (1.15 g, 10 mmol) /$CuCO_3$ (1.24 g, 10 mmol) were stirred for about 30 minutes, respectively. The clear solutions were allowed to stand at room temperature for slow evaporation. After about one week, colorless and blue crystals of $(C_6H_{14}N_2)[Mn(H_2O)_6][SiF_6]_2$ (**1-Mn**)and $(C_6H_{14}N_2)[Cu(H_2O)_6][SiF_6]_2$ (**1-Cu**) were obtained in about 85% and 82% yield based on Mn and Cu, respectively. The phase purity of **1-Mn** and **1-Cu** were verified by infrared (IR) spectra measurements (Fig. S1) and powder X-Ray diffraction patterns which matching well with the simulated one in terms of the single-crystal structures (Fig. S2). Elemental analyses: For **1-Mn** calcd C: 12.84%, N: 4.99%, H: 4.67%; found C: 13.04%, N: 5.06%, H: 4.64%. For **1-Cu** calcd C: 12.67%, N: 4.93%, H: 4.37%; found C: 12.77%, N: 4.76%, H: 4.52%.

Table S1. Summary of crystallographic data and structural refinements for **1-Mn** and **1-Cu** at 173 and 293 K.

Empirical formula	$(C_6H_{14}N_2)[Mn(H_2O)_6][SiF_6]_2$		$(C_6H_{14}N_2)[Cu(H_2O)_6][SiF_6]_2$	
Formula weight	561.40		569.99	
T / K	173	293	173	293
Phase	LTP	HTP	LTP	HTP
Space group	*R*32	$R\bar{3}c$	*C*2/*c*	$R\bar{3}c$
a / Å	9.330(3)	9.457(1)	15.9780(2)	9.3490(9)
b / Å	9.330(3)	9.457(1)	27.7885(3)	9.3490(9)
c / Å	38.34(1)	38.660(8)	38.1976(5)	38.422(5)
α / *degree*	90	90	90	90
β / *degree*	90	90	90.264(1)	90
γ / *degree*	120	120	90	120
V / Å^3	2890(2)	2994(1)	16959.7(4)	2908.3(7)
Z	6	6	36	6
GOF	1.101	1.174	1.229	1.099
R_1, wR_2 [$I > 2\sigma(I)$][a]	0.0332, 0.0880	0.0595, 0.1516	0.0400, 0.0865	0.0532, 0.1626
R_1, wR_2 (all data)	0.0340, 0.0889	0.0618, 0.1549	0.0462, 0.0883	0.0547, 0.1643
Flack parameter	0.42(4)	–	–	–

[a] $R_1 = F_o - F_c/F_o$, $wR_2 = \{w[(F_o)^2 - (F_c)^2]^2/w[(F_o)^2]^2\}^{1/2}$

Table S2. The selected bond lengths (Å) of **1-Mn** and **1-Cu** at 173 and 293 K.

1-Mn	173 K	Mn1–O1	2.141(2)	Mn1–O1^{1}	2.141(2)
		Mn1–O1^{2}	2.141(2)	Mn–O2	2.166(2)
		Mn–O2^{1}	2.166(2)	Mn–O2^{2}	2.166(2)
	293 K	Mn1–O1	2.146(3)	Mn1–O1^{1}	2.146(3)
		Mn1–O1^{2}	2.146(3)	Mn1–O1^{3}	2.146(3)
		Mn1–O1^{4}	2.146(3)	Mn1–O1^{5}	2.146(3)
1-Cu	173 K	Cu1–O1	1.997(2)	Cu1–O1^{1}	1.997(2)
		Cu1–O2	2.247(2)	Cu1–O2^{1}	2.247(2)
		Cu1–O3	1.967(2)	Cu1–O3^{1}	1.967(2)
		Cu2–O4	2.017(2)	Cu2–O5	1.984(2)
		Cu2–O6	2.256(2)	Cu2–O7	1.993(2)
		Cu2–O8	1.981(2)	Cu2–O9	2.251(2)
		Cu3–O10	1.973(2)	Cu3–O11	2.010(2)
		Cu3–O12	2.232(2)	Cu3–O13	1.990(2)
		Cu3–O14	2.044(2)	Cu3–O15	2.229(2)
		Cu4–O16	1.994(2)	Cu4–O17	1.979(2)
		Cu4–O18	2.231(2)	Cu4–O19	1.995(2)
		Cu4–O20	1.968(2)	Cu4–O21	2.245(2)
		Cu5–O22	1.983(2)	Cu5–O23	2.237(2)
		Cu5–O24	2.012(2)	Cu5–O25	2.040(2)
		Cu5–O25	2.229(2)	Cu5–O27	1.973(2)
	293 K	Cu1–O1	2.046(3)	Cu1–O1^{1}	2.045(3)
		Cu1–O1^{2}	2.045(3)	Cu1–O1^{3}	2.045(4)
		Cu1–O1^{4}	2.045(3)	Cu1–O1^{5}	2.045(4)

Symmetry code

1-Mn

173 K: ^{1}1-*y*, +*x*-*y*, +*z*; ^{2}1+*y*-*x*, 1-*x*, +*z*;

293 K: ^{1}4/3-*x*, 2/3-*y*, 5/3-*z*; ^{2}1/3-*y*+*x*, -1/3+*x*, 5/3-*z*; ^{3}1/3+*y*, 2/3-*x*+*y*, 5/3-*z*; ^{4}1-*y*, +*x*-*y*, +*z*; ^{5}1+*y*-*x*, 1-*x*, +*z*;

1-Cu

173 K: ^{1}1-*x*, -*y*, 1-*z*;

293 K: ^{1}1-*y*, +*x*-*y*, +*z*; ^{2}1/3+*y*, 2/3-*x*+*y*, 5/3-*z*; ^{3}1+*y*-*x*, 1-*x*, +*z*; ^{4}4/3-*x*, 2/3-*y*, 5/3-*z*; ^{5}1/3-*y*+*x*, -1/3+*x*, 5/3-*z*;

Table S3. The selected bond angles (°) of **1-Mn** and **1-Cu** at 173 and 293 K.

1-Mn	173 K	∠O1–Mn1–O1^1	88.33(9)	∠O1–Mn1–O1^2	88.33(9)
		∠O1–Mn1–O2	88.37(9)	∠O1–Mn1–O2^1	175.5(1)
		∠O1–Mn1–O2^2	94.6(1)	∠O1^1–Mn1–O1^2	88.33(9)
		∠O1^1–Mn1–O2	94.6(1)	∠O1^1–Mn1–O2^1	88.37(9)
		∠O1^1–Mn1–O2^2	175.5(1)	∠O1^2–Mn1–O2	175.5(1)
		∠O1^2–Mn1–O2^1	94.6(1)	∠O1^2–Mn1–O2^2	88.37(9)
		∠O2–Mn1–O2^1	88.89(8)	∠O2–Mn1–O2^2	88.89(8)
		∠O2^1–Mn1–O2^2	88.89(8)		
	293 K	∠O1–Mn1–O1^1	180.0	∠O1–Mn1–O1^2	91.8(1)
		∠O1–Mn1–O1^3	88.3(10)	∠O1–Mn1–O1^4	88.3(1)
		∠O1–Mn1–O1^5	91.8(1)	∠O1^1–Mn1–O1^2	88.2(1)
		∠O1^1–Mn1–O1^3	91.8(1)	∠O1^1–Mn1–O1^4	91.8(1)
		∠O1^1–Mn1–O1^5	88.3(1)	∠O1^2–Mn1–O1^3	91.8(1)
		∠O1^2–Mn1–O1^4	180.0(2)	∠O1^2–Mn1–O1^5	88.3(1)
		∠O1^3–Mn1–O1^4	88.3(1)	∠O1^3–Mn1–O1^5	180.0(2)
		∠O1^4–Mn1–O1^5	91.8(1)		
1-Cu	173 K	∠O1–Cu1–O1^1	180.0(2)	∠O1–Cu1–O2	90.77(9)
		∠O1–Cu1–O2^1	89.23(9)	∠O1–Cu1–O3	88.66(9)
		∠O1–Cu1–O3^1	91.34(9)	∠O1^1–Cu1–O2	89.23(9)
		∠O1^1–Cu1–O2^1	90.77(9)	∠O1^1–Cu1–O3	91.34(9)
		∠O1^1–Cu1–O3^1	88.66(9)	∠O2–Cu1–O2^1	180.0(1)
		∠O2–Cu1–O3	89.97(9)	∠O2–Cu1–O3^1	90.03(9)

∠O2[1]–Cu1–O3	90.03(9)	∠O2[1]–Cu1–O3[1]	89.97(9)
∠O3–Cu1–O3[1]	180.0(1)	∠O4–Cu2–O5	90.54(9)
∠O4–Cu2–O6	89.67(8)	∠O4–Cu2–O7	179.00(9
∠O4–Cu2–O8	90.55(9)	∠O4–Cu2–O9	88.15(8)
∠O5–Cu2–O6	91.07(8)	∠O5–Cu2–O7	88.72(9)
∠O5–Cu2–O8	178.28(9)	∠O5–Cu2–O9	91.37(8)
∠O6–Cu2–O7	89.67(9)	∠O6–Cu2–O8	90.27(8)
∠O6–Cu2–O9	176.74(8)	∠O7–Cu2–O8	90.20(9)
∠O7–Cu2–O9	92.54(8)	∠O8–Cu2–O9	87.33(9)
∠O10–Cu3–O11	90.27(9)	∠O10–Cu3–O12	90.34(9)
∠O10–Cu3–O13	178.04(9)	∠O10–Cu3–O14	90.71(9)
∠O10–Cu3–O15	87.35(9)	∠O11–Cu3–O12	89.16(9)
∠O11–Cu3–O13	88.56(9)	∠O11–Cu3–O14	177.95(9)
∠O11–Cu3–O15	93.60(9)	∠O12–Cu3–O13	91.21(9)
∠O12–Cu3–O14	89.03(9)	∠O12–Cu3–O15	176.41(8)
∠O13–Cu3–O14	90.50(8)	∠O13–Cu3–O15	91.15(8)
∠O14–Cu3–O15	88.25(9)	∠O16–Cu4–O17	91.26(9)
∠O16–Cu4–O18	92.36(9)	∠O16–Cu4–O19	88.74(9)
∠O16–Cu4–O20	178.66(9)	∠O16–Cu4–O21	88.21(8)
∠O17–Cu4–O18	89.50(9)	∠O17–Cu4–O19	179.4(1)
∠O17–Cu4–O20	89.43(9)	∠O17–Cu4–O21	89.09(9)
∠O18–Cu4–O19	89.86(9)	∠O18–Cu4–O20	88.79(9)
∠O18–Cu4–O21	178.49(9)	∠O19–Cu4–O20	90.58(9)

	∠O19–Cu4–O21	91.55(9)	∠O20–Cu4–O21	90.65(9)
	∠O22–Cu5–O23	91.43(8)	∠O22–Cu5–O24	88.52(9)
	∠O22–Cu5–O25	90.51(9)	∠O22–Cu5–O26	90.91(8)
	∠O22–Cu5–O27	178.34(9)	∠O23–Cu5–O24	92.83(9)
	∠O23–Cu5–O25	88.40(8)	∠O23–Cu5–O26	176.65(8)
	∠O23–Cu5–O27	87.11(8)	∠O24–Cu5–O25	178.45(9)
	∠O24–Cu5–O26	89.62(9)	∠O24–Cu5–O27	90.76(9)
	∠O25–Cu5–O26	89.18(9)	∠O25–Cu5–O27	90.24(9)
	∠O26–Cu5–O27	90.58(9)		
293 K	∠O1–Cu1–O1^{1}	89.6(1)	∠O1–Cu1–O1^{2}	89.6(1)
	∠O1–Cu1–O1^{3}	90.4(1)	∠O1–Cu1–O1^{4}	90.4(1)
	∠O1–Cu1–O1^{5}	180.0	∠O1^{1}–Cu1–O1^{2}	89.6(1)
	∠O1^{1}–Cu1–O1^{3}	180.0	∠O1^{1}–Cu1–O1^{4}	90.4(1)
	∠O1^{1}–Cu1–O1^{5}	90.4(1)	∠O1^{2}–Cu1–O1^{3}	90.4(1)
	∠O1^{2}–Cu1–O1^{4}	180.0	∠O1^{2}–Cu1–O1^{5}	90.4(1)
	∠O1^{3}–Cu1–O1^{4}	89.6(1)	∠O1^{3}–Cu1–O1^{5}	89.6(1)
	∠O1^{4}–Cu1–O1^{5}	89.6(1)		

Symmetry code

1-Mn

173 K: ^{1}1-*y*, +*x*-*y*, +*z*; ^{2}1+*y*-*x*, 1-*x*, +*z*;

293 K: ^{1}4/3-*x*, 2/3-*y*, 5/3-*z*; ^{2}1/3+*y*, 2/3-*x*+*y*, 5/3-*z*; ^{3}1+*y*-*x*, 1-*x*, +*z*; ^{4}1-*y*, +*x*-*y*, +*z*; ^{5}1/3-*y*+*x*, -1/3+*x*, 5/3-*z*;

1-Cu

173 K: ^{1}1-*x*, -*y*, 1-*z*; ^{2}1-*x*, +*y*, 1/2-*z*;

293 K: ^{1}1-*y*, +*x*-*y*, +*z*; ^{2}1+*y*-*x*, 1-*x*, +*z*; ^{3}1/3+*y*, 2/3-*x*+*y*, 5/3-*z*; ^{4}1/3-*y*+*x*, -1/3+*x*, 5/3-*z*; ^{5}4/3-*x*, 2/3-*y*, 5/3-*z*;

Table S4. The geometry (Å, °) of hydrogen bonds for **1-Mn** and **1-Cu** at 173 and 293 K.

		D–H···A	D–H	H···A	D···A	∠D–H···A
1-Mn	173 K	N1–H1···F4^{1}	0.980	2.125	2.947	140.38
		N1–H1···F4^{2}	0.980	2.125	2.947	140.39
		N1–H1···F4^{3}	0.980	2.125	2.947	140.38
		N2–H2···F1^{4}	0.980	2.119	2.939	140.19
		N2–H2···F1^{5}	0.980	2.118	2.939	140.19
		N2–H2···F1^{6}	0.980	2.119	2.939	140.19
		O1–H1A···F3^{7}	0.848	2.513	2.994	116.94
		O1–H1A···F4^{8}	0.848	1.846	2.693	177.72
		O1–H1B···F3	0.834	1.900	2.682	155.80
		O2–H2A···F2^{9}	0.845	2.518	2.995	116.75
		O2–H2A···F1^{10}	0.845	1.898	2.726	165.97
		O2–H2B···F2	0.840	1.888	2.721	171.25
	293 K	N1–H1···F2	0.980	2.133	2.956	140.49
		N1–H1···F2^{1}	0.980	2.133	2.956	140.50
		N1–H1···F2^{2}	0.980	2.133	2.956	140.49
		N1–H1···F2’	0.980	2.145	2.974	141.39
		N1–H1···F2’^{1}	0.980	2.145	2.974	141.39
		N1–H1···F2’^{2}	0.980	2.145	2.974	141.39
		O1–H1C···F1^{3}	0.854	1.855	2.703	171.97
		O1–H1C···F1’^{3}	0.854	2.003	2.709	139.40
		O1–H1C···F1’^{4}	0.854	2.514	3.304	154.22
		O1–H1D···F2’^{4}	0.854	2.257	2.745	116.38
1-Cu	173 K	N1–H1–F31^{1}	1.000	2.026	2.901	144.90
		N1–H1–F33^{1}	1.000	2.362	3.109	130.82
		N1–H1–F35^{1}	1.000	2.008	2.856	141.12
		N2-H2–F8	1.000	2.204	3.021	137.90
		N2-H2–F10	1.000	2.128	2.964	139.88
		N2-H2–F11	1.000	2.066	2.919	141.90
		N3-H3–F4	1.000	2.156	2.949	134.98
		N3-H3–F5	1.000	1.947	2.848	148.41
		N3-H3–F6	1.000	2.249	3.031	134.00
		N4-H4–F21	1.000	2.228	3.020	135.11
		N4-H4–F22	1.000	2.023	2.891	143.80
		N4-H4–F23	1.000	2.084	2.915	139.19

N5-H5–F49[2]	1.000	2.162	2.994	139.54
N5-H5–F50[2]	1.000	2.245	3.033	134.63
N5-H5–F53[2]	1.000	1.973	2.847	144.51
N6-H6–F25[3]	1.000	2.172	2.992	138.15
N6-H6–F26[3]	1.000	2.057	2.910	141.92
N6-H6–F30[3]	1.000	2.118	2.944	138.65
N7-H7–F13[4]	1.000	2.227	3.026	135.84
N7-H7–F14[4]	1.000	2.159	2.973	137.45
N7-H7–F15[4]	1.000	2.020	2.904	146.17
N8-H8–F43	1.000	2.185	3.001	137.71
N8-H8–F47	1.000	2.070	2.909	140.12
N8-H8–F48	1.000	2.095	2.936	140.45
N9-H9–F39	1.000	2.265	3.035	132.86
N9-H9–F40	1.000	1.956	2.827	144.07
N9-H9–F41	1.000	2.128	2.970	140.72
O15-H15C–F28	0.807	1.956	2.742	164.58
O15-H15C–F28[3]	0.807	2.573	2.973	112.21
O10-H10A–F18	0.728	1.959	2.682	171.32
O27-H27A–F37[3]	0.796	2.599	3.053	117.85
O27-H27A–F39[3]	0.796	1.881	2.675	175.49
O24-H24C–F51	0.806	1.855	2.655	171.12
O22-H22C–F45[5]	0.821	2.521	2.971	115.69
O22-H22C–F47[5]	0.821	1.910	2.725	171.45
O19-H19C–F49[3]	0.821	1.886	2.704	174.59
O19-H19C–F54[3]	0.821	2.636	3.091	116.51
O6-H6C–F41[6]	0.818	1.933	2.750	175.69
O6-H6C–F42[6]	0.818	2.600	3.093	120.13
O12-H12A–F23	0.771	1.980	2.749	175.73
O12-H12A–F24	0.771	2.561	3.032	121.14
O13-H13C–F27	0.838	1.846	2.671	167.72
O22-H22D–F45	0.794	1.902	2.691	172.13
O24-H24D–F22[5]	0.746	1.918	2.661	173.66
O14-H14C–F29	0.789	1.944	2.705	162.32
O15-H15D–F28[3]	0.792	2.520	2.973	117.84
O15-H15D–F30[3]	0.792	2.005	2.781	166.41
O23-H23C–F27	0.866	2.526	2.947	110.81
O23-H23C–F46	0.866	1.919	2.761	163.51

O27-H27B–F54	0.805	1.880	2.677	170.37
O7-H7A–F5[3]	0.752	1.933	2.662	163.11
O26-H26A–F52	0.808	1.968	2.745	161.10
O11-H11A–F40	0.833	1.847	2.678	175.23
O4-H4C–F8[5]	0.752	2.059	2.761	155.62
O4-H4C–F9[5]	0.752	2.637	3.045	116.19
O26-H26B–F1[7]	0.766	2.586	3.024	118.10
O26-H26B–F4[7]	0.766	2.009	2.770	172.81
O6-H6D–F34[6]	0.840	1.908	2.739	169.84
O10-H10B–F3	0.909	2.589	3.081	114.65
O10-H10B–F6	0.909	1.789	2.693	172.53
O8-H8A–F19[5]	0.834	2.625	3.050	113.07
O8-H8A–F21[5]	0.834	1.856	2.685	172.74
O5-H5C–F43[6]	0.799	1.957	2.731	163.14
O5-H5C–F44[6]	0.799	2.500	2.990	120.96
O7-H7B–F32[6]	0.864	1.783	2.642	173.05
O8-H8B–F36[6]	0.788	1.897	2.676	169.58
O9-H9A–F29	0.805	2.525	2.957	115.07
O9-H9A–F12	0.805	1.999	2.766	159.22
O1-H1C–F32[8]	0.817	2.528	2.922	110.91
O1-H1C–F33[8]	0.817	1.931	2.743	172.05
O1-H1C–F15	0.865	1.906	2.765	172.05
O12-H12B–F16	0.742	2.005	2.739	169.77
O4-H4D–F9	0.818	1.909	2.721	172.16
O20-H20C–F34	0.769	2.624	3.043	116.15
O20-H20C–F35	0.769	1.911	2.680	176.56
O14-H14D–F10	0.832	1.977	2.791	165.95
O18-H18C–F3[9]	0.874	1.878	2.751	175.96
O18-H18C–F36[9]	0.874	2.606	3.067	113.92
O17-H17C–F14[4]	0.775	1.928	2.701	176.29
O17-H17C–F16[4]	0.775	2.617	3.088	120.92
O3-H3C–F53[2]	0.837	1.862	2.696	174.58
O21-H21C–F13	0.808	2.030	2.835	174.20
O21-H21C–F17	0.808	2.549	2.959	112.85
O11-H11B–F17	0.899	1.753	2.645	171.32
O1-H1D–F2	0.818	1.911	2.715	167.69
O18-H18D–F19[1]	0.712	2.002	2.695	164.93

	O2-H2D–F3	0.678	2.028	2.694	167.19
	O16-H16C–F20[1]	0.816	1.898	2.700	167.44
	O21-H21D–F38	0.767	1.999	2.733	159.91
	O20-H20D–F42	0.795	1.850	2.638	170.97
	O3-H3D–F1[10]	0.835	1.814	2.630	165.50
	O16-H16D–F50[2]	0.854	1.904	2.758	177.65
	O16-H16D–F51[2]	0.854	2.499	2.988	117.20
	O9-H9B–F25	0.835	1.945	2.774	171.41
	O9-H9B–F29	0.835	2.499	2.957	115.52
	O13-H13D–F46	0.769	2.571	3.007	117.77
	O13-H13D–F48	0.769	2.024	2.744	155.76
	O19-H19D–F37	0.732	1.936	2.662	170.90
	O5-H5D–F7[6]	0.734	1.958	2.690	175.74
	O25-H25A–F44	0.794	1.950	2.733	168.36
	O25-H25B–F7[6]	0.856	2.500	3.033	121.15
	O25-H25B–F11[6]	0.856	1.952	2.775	160.78
	O17-H17D–F24[1]	0.806	1.853	2.643	166.17
	O23-H23D–F26	0.764	2.053	2.784	160.13
	O23-H23D–F27	0.764	2.540	2.947	115.16
293 K	O1-H1C–F2'[1]	0.867	2.182	2.741	121.92
	O1-H1D–F1	0.867	1.881	2.676	151.62
	O1-H1D–F1'	0.867	2.418	3.235	157.37
	O1-H1D–F1'[2]	0.867	2.279	2.766	115.55
	N1-H1–F2	0.980	2.137	2.959	140.44
	N1-H1–F2[3]	0.980	2.137	2.959	140.44
	N1-H1–F2[2]	0.980	2.137	2.959	140.44

Symmetry code:

1-Mn

173 K: [1]*x*-*y*+2/3, -*y*+4/3, -*z*+1/3; [2]-*x*+5/3, -*x*+*y*+4/3, -*z*+1/3; [3]*y*+2/3, *x*+1/3, -*z*+1/3; [4]*x*-*y*, -*y*+1, -*z*; [5]-*x*+1, -*x*+*y*+1, -*z*; [6]*y*, *x*, -*z*; [7]*y*+2/3, *x*-2/3, -*z*+1/3; [8]*x*-*y*+2/3, -*y*+1/3, -*z*+1/3; [9]-*x*+2, -*x*+*y*+1, -*z*; [10]*x*-*y*+1, -*y*+1, -*z*;

293 K: [1]-*y*+1, *x*-*y*, *z*; [2]-*x*+*y*+1, -*x*+1, *z*; [3]*y*+1/3, -*x*+*y*+2/3, -*z*+5/3; [4]*x*+1/3, *x*-*y*+2/3, *z*+1/6;

1-Cu

173 K: 1-*x*+3/2, -*y*+1/2, -*z*+1; 2*x*-1/2, -*y*+1/2, *z*+1/2; 3-*x*+1, *y*, -*z*+1/2; 4-*x*+3/2, -*y*+1/2, -*z*+1; 5-*x*+2, *y*, -*z*+1/2; 6-*x*+3/2, *y*-1/2, -*z*+1/2; 7-*x*+3/2, *y*+1/2, -*z*+1/2; 8*x*-1/2, *y*-1/2, *z*; 9-*x*+1, -*y*+1, -*z*+1; 10-*x*+1, -*y*, -*z*+1;

293 K: [1]*y*, *x*, -*z*+3/2; [2]-*x*+*y*+1, -*x*+1, *z*; [3]-*y*+1, *x*-*y*, *z*

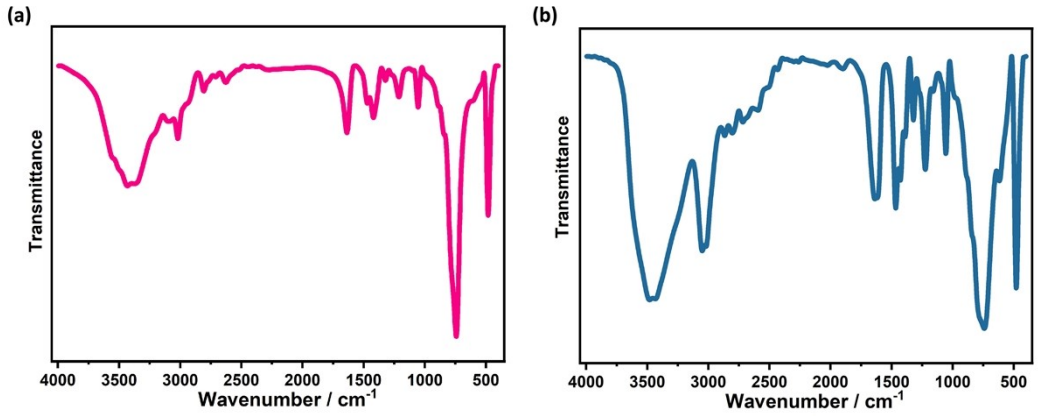

Fig S1 IR spectra of **1-Mn** (a) and **1-Cu** (b).

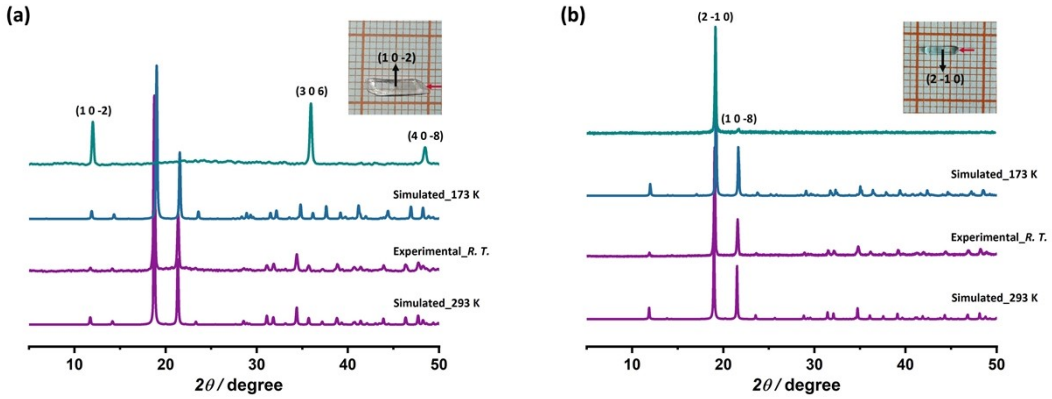

Fig. S2 The powder XRD patterns of **1-Mn** (a) and **1-Cu** (b) for the simulated at 173 K and 293 K, experimental at room temperature, and single crystals of the largest face (black arrows), respectively.

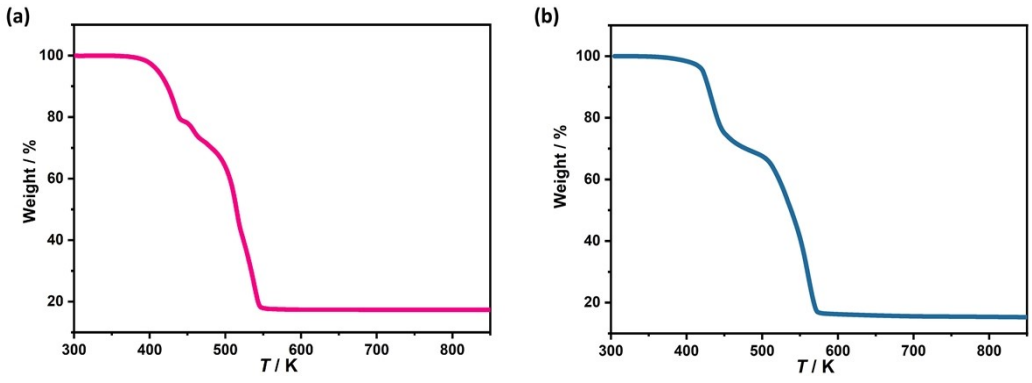

Fig. S3 TG curves measured at a rate of 5 K/min under N_2 atmosphere show that **1-Mn** (a) and **1-Cu** (b) can be stable up to about 363 K.

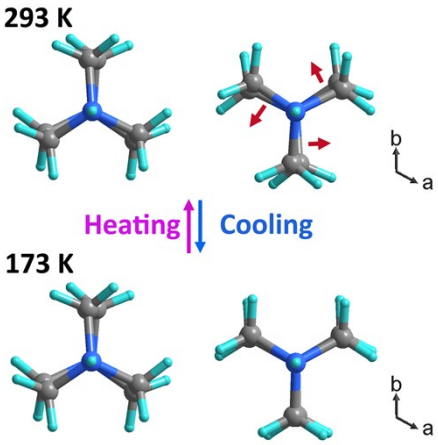

Fig. S4 Twisting motion of the $(H_2dabco)^+$ cations for **1-Mn**. The asymmetric units of 293 and 173 K contain one $(H_2dabco)^+$ cation and two $(H_2dabco)^+$ cations, respectively. From 293 K to 173 K, the $(H_2dabco)^+$ cations exhibit obvious twisting motion (red arrows) along the *c*-axis.

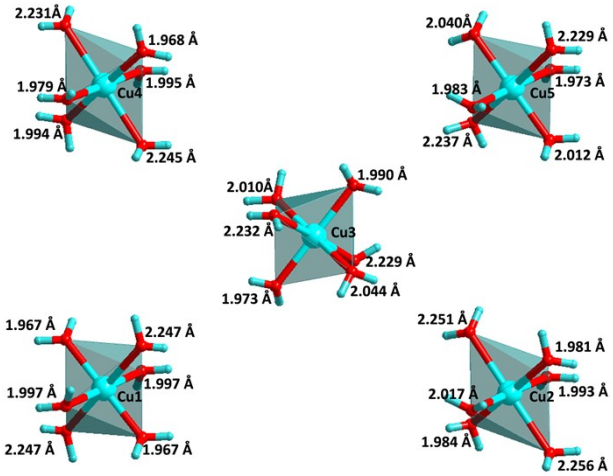

Fig. S5 The five different $[Cu(H_2O)_6]^{2+}$ octahedra of **1-Cu** at 173 K.

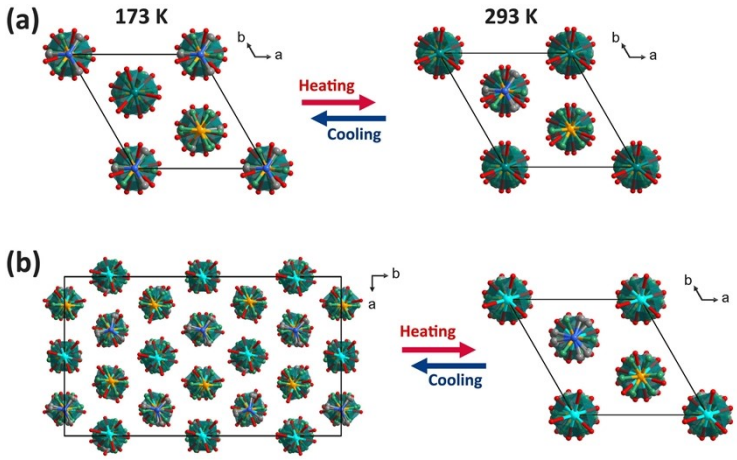

Fig. S6 The packing structures viewed along the *c*-axis of **1-Mn** (a) and **1-Cu** (b) at 173 and 293 K.

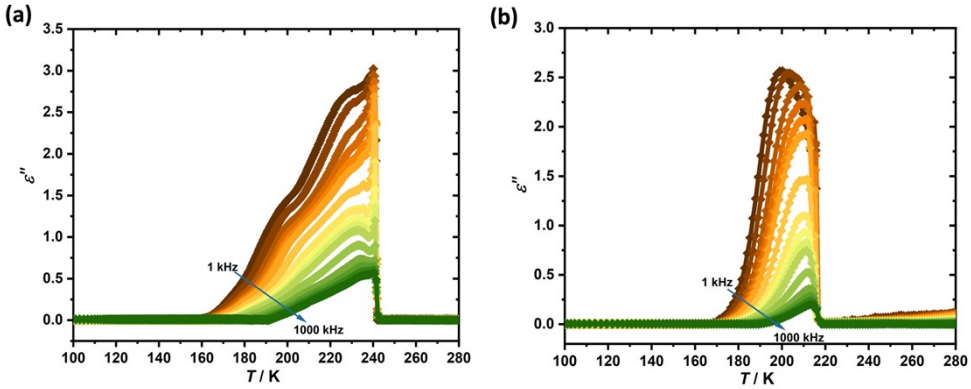

Fig. S7 Imaginary part (ε'') of the dielectric permittivity of **1-Mn** (a) and **1-Cu** (b) as a function of temperature at various frequencies from 1 kHz to 1000 kHz on a cooling process measured with single crystals along to largest face (black arrows in the inset of Fig. S2).

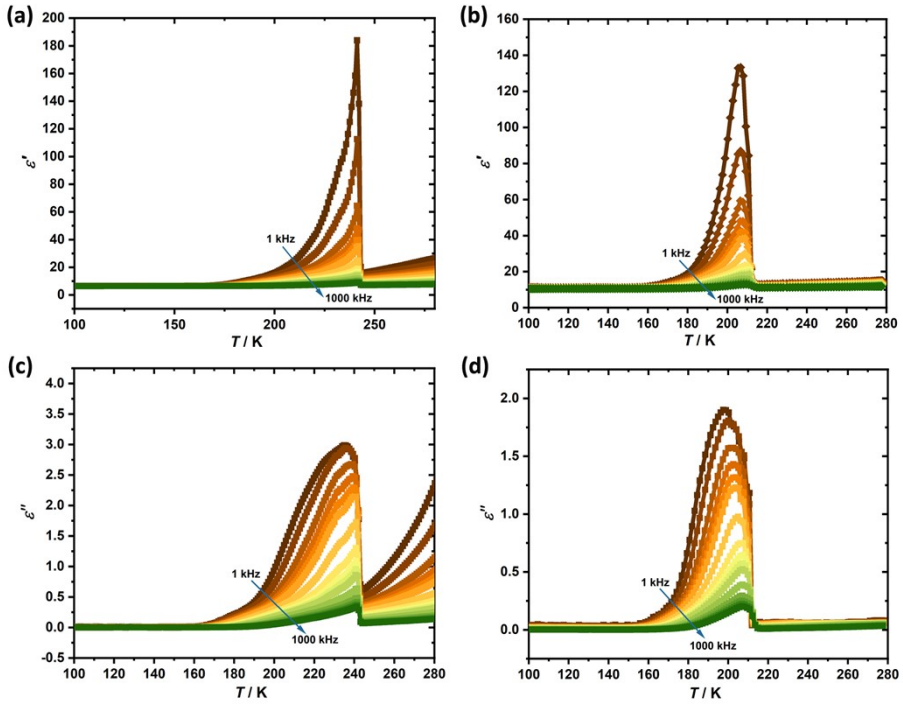

Fig. S8 Real part (ε') and imaginary part (ε'') of the dielectric permittivity of **1-Mn** (a & c) and **1-Cu** (b & d) as a function of temperature at various frequencies from 1 kHz to 1000 kHz on a cooling process measured with single crystals perpendicular to largest face (red arrows in the inset of Fig. S2).

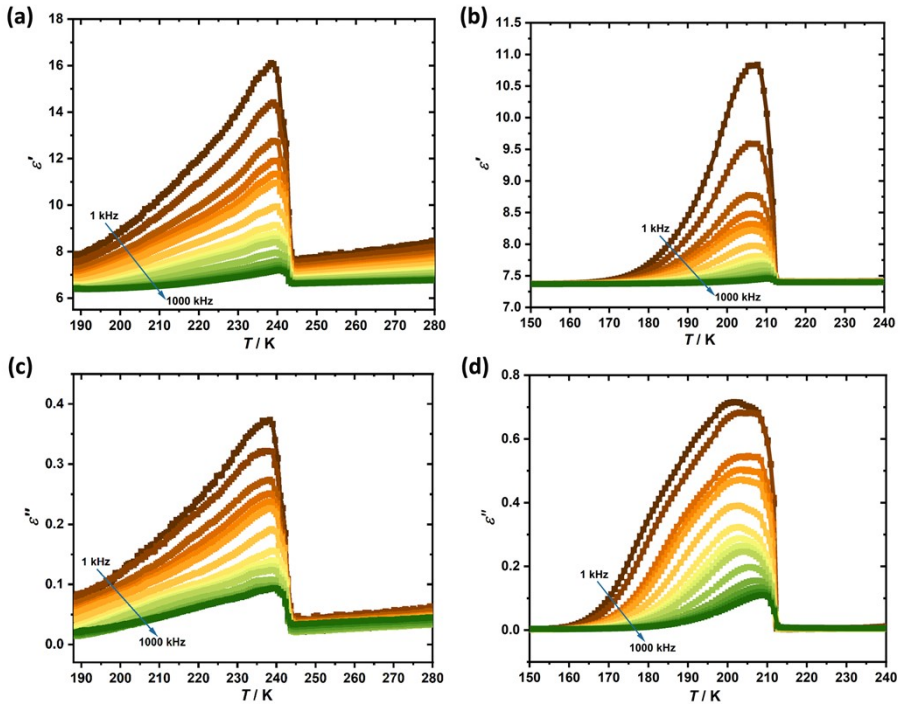

Fig. S9 Real part (ε') and imaginary part (ε'') of the dielectric permittivity of **1-Mn** (a & c) and **1-Cu** (b & d) as a function of temperature at various frequencies from 1 kHz to 1000 kHz on a cooling process measured with powder-pressed samples.

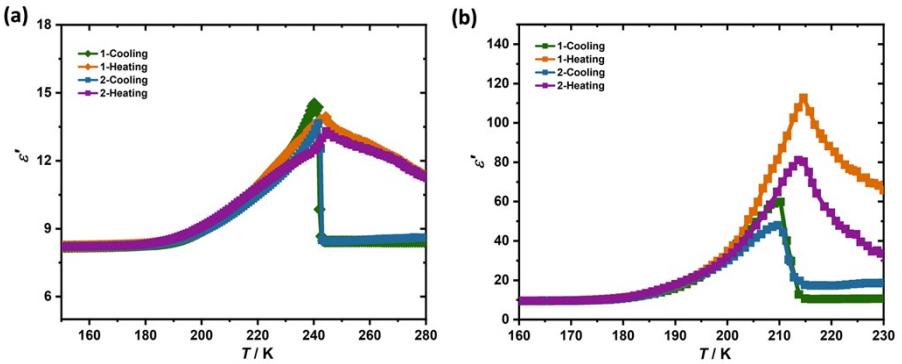

Fig. S10 Two heating-cooling cycles of the dielectric constant of **1-Mn** (a, 1000 kHz) and **1-Cu** (b, 4 kHz) as a function of temperature.